

Multiple resonant Raman scattering with spin flip and trapping of 29 cm^{-1} acoustic phonons in ruby in a magnetic field

S. A. Basun, A. A. Kaplyanskiĭ, and V. L. Shekhtman

A. F. Ioffe Physicotechnical Institute, USSR Academy of Sciences

(Submitted 22 July 1981; resubmitted 15 February 1982)

Zh. Eksp. Teor. Fiz. **82**, 1945–1963 (June 1982)

The influence of an external magnetic field H on the trapping of 29 cm^{-1} acoustic phonons multiply scattered resonantly in electronic $\bar{E}-2\bar{A}$ transitions in the metastable state of Cr^{3+} ions in ruby is investigated in detail. An anomalous nonmonotonic dependence of the degree of trapping on H is observed. It is attributed to inelastic scattering of the phonons with production (absorption) of a Zeeman \bar{E} -level quantum (resonant Raman scattering of phonons with spin flip). A theory of multiple resonant Raman scattering of phonons in a magnetic field is developed, and the probabilities of the $\bar{E}-2\bar{A}$ transitions with and without spin flip are determined by comparing this theory with experiment.

PACS numbers: 78.30.Gt, 78.20.Ls, 71.70.Ej, 71.38. + i

Resonant trapping of acoustic 29 cm^{-1} (0.87 THz) phonons in crystals of optically excited ruby $\text{Al}_2\text{O}_3:\text{Cr}^{3+}$ has been actively investigated the last few years. The trapping of the phonons is due to a multiple resonant scattering by Cr^{3+} ions in the metastable $\bar{E}(^2E)$ state; the scattering is due to the resonant interaction of the 29 cm^{-1} phonons with the pair of electron levels \bar{E} and $2\bar{A}$. The phonon trapping in ruby is of great general interest, and its mechanism^{4,6-8} differs in principle from the known mechanism of radiation trapping in gases.^{9,10}

In experiments on optical detection of phonons²⁻⁵ the degree of trapping of the phonons is registered by means of the radiation in the R_2 line of ruby. The kinetics of the R_2 radiation is investigated in nonstationary experiments,^{2,5} and its intensity in stationary ones.³ The resonant scattering of the 29 cm^{-1} phonons takes place in the optically excited volume of the crystal. The nonequilibrium phonons are injected into this volume either from the outside (in experiments with thermal pulses²) or "from within" (in the $2\bar{A}-\bar{E}$ relaxation following optical excitation of the ions^{3,5}).

Experiments with thermal pulses¹¹ have revealed, for the first time ever, a shortening of the phonon trapping time in the excited volume under the influence of an external magnetic field. The effect was attributed to Zeeman splitting of the Kramers levels \bar{E} and $2\bar{A}$, which leads to splitting of the line of the $\bar{E}-2\bar{A}$, which leads to splitting of the line of the $\bar{E}-2\bar{A}$ phonon transition and accordingly to a decrease of the spectral cross section for the scattering. Phonon trapping in a magnetic field was subsequently investigated both under nonstationary^{8,10} and stationary^{3,4,13} experimental conditions. In addition to the already mentioned "bleaching" of the volume in the field, the "spectral diffusion" of the phonons was also considered.^{3,6,13}

In the present study (see also the brief communications^{14,15}) we have observed and investigated in detail the anomalous dependence of the 29 cm^{-1} phonon trapping on the external magnetic field (Sec. 1). The anomaly consists in the fact that with increasing field, on

going through a threshold value $H=0.6\text{ kOe}$, enhancement of the trapping sets in, so that on the whole the dependence of the degree of imprisonment on the field intensity is nonmonotonic. The interpretation of the phenomenon is based on a development of an earlier theory^{6,7} of trapping of resonant phonons in ruby (Sec. 3). Anomalous trapping in a magnetic field is attributed to the influence of inelastic phonon scattering with production (absorption) of the \bar{E} -level Zeeman quantum [resonant Raman scattering (RRS) of the phonons with spin flip; Sec. 3]. A phonon-multiple-scattering theory that takes into account elastic resonant scattering and RRS is considered and used as a basis for a quantitative explanation of the results (Sec. 4). From a comparison of the theory with experiment we determine a number of microparameters of the system, including the ratio of the probabilities of the $\bar{E}-2\bar{A}$ phonon transitions with and without spin flip (Sec. 5). The Appendix deals with the decisive role of the RRS of the phonons in the Orbach-Aminov spin relaxation^{16,17} of the \bar{E} level at low temperatures (Sec. 6).

1. EXPERIMENTAL PART

We used a stationary-luminescence method³ wherein the relative intensity $\eta = R_2/R_1$ of ruby-radiation R lines is measured at different powers W of stationary optical excitation (i. e., at different densities N^* of the chromium ions in the metastable \bar{E} state). We used moderate pumping powers W , at which the density N^* did not exceed 10^{17} cm^{-3} . Under these conditions, the nonequilibrium 29 cm^{-1} phonons are produced mainly in $2\bar{A}-\bar{E}$ transitions in the course of relaxation of the Cr^{3+} ions following their optical excitation to high-energy states. The value of η is governed by the emission of the optical R_2 photons (with probability $\sim 10^{-6}$) in rescattering of the phonons in the excited volume, as well as by the hot and equilibrium R_2 luminescence.^{3,4} It follows from balance considerations that

$$\eta = \frac{f_2}{f_1} \left[\beta \frac{T}{\tau_{R_1}} (1+M) + \bar{n}_0 \right], \quad (1)$$

where f_2/f_1 is the ratio of the oscillator strengths of the

lines R_2 and R_1 in the given experimental geometry; T is the lifetime of the $2\bar{A}$ level relative to spontaneous decay $2\bar{A} \rightarrow \bar{E}$ with emission of 29 cm^{-1} phonons ($\sim 1 \text{ nsec}$); τ_{R_1} is the radiative lifetime of the \bar{E} level ($\sim 4 \text{ msec}$); $\beta = \Lambda_{2\bar{A}} / (\Lambda_{2\bar{A}} + \Lambda_{\bar{E}})$ is branching coefficient of the pumping of the levels $2\bar{A}$ and \bar{E} upon relaxation from the higher states; $\bar{n}_0 = (e^{42/T} - 1)^{-1}$ is the occupation number of the equilibrium 29 cm^{-1} phonons at the crystal temperature T ; M is the number of rescatterings of the relaxation 29 cm^{-1} , averaged over the volume and over the spectral contour of the phonon $2\bar{A} \rightarrow \bar{E}$ line during the time of the phonon stay in the excited volume. Since the observed quantity η depends explicitly on M_1 , it serves as a quantitative measure of the degree of imprisonment of the 29 cm^{-1} phonons.

The measurements were made on an oriented single crystal of $\text{Al}_2\text{O}_3 : 0.02\% \text{ Cr}^{3+}$ measuring $2 \times 3 \times 10 \text{ mm}$ at temperatures 1.8 and 4.2 K. The sample was in a homogeneous magnetic field $H \parallel C_3$ (C_3 is the trigonal axis of the crystal) of a superconducting solenoid (Fig. 1a). The field intensity ranged from zero to 3.5 kOe. The optical excitation was produced by a "Spectra Physics" argon laser, model 164-05, with beam diameter $d \approx 1.3 \text{ mm}$ and power up to 1 W in the 514.5 nm line. The beam was directed in the sample perpendicular to C_3 . The laser-excited ruby radiation was extracted from the cryostat with a light pipe and projected on the slit of a DFS-24 grating double monochromator, which separated the R_2 and R_1 luminescence lines. The detector was an FÉU-79 photomultiplier in the photon counting regime, followed by amplification and discrimination of the single-electron pulses. Since η ranged from 10^{-6} to 10^{-4} , depending on the laser power W , the radiation was attenuated with calibrated neutral filters.

The dependence of η on the field was investigated at pump powers W corresponding to variation of N^* in the interval $10^{15} - 10^{17} \text{ cm}^{-3}$. Figure 1 shows the measured field dependence, normalized to $H=0$, of the intensity of $R_2(H)/R_2(0)$ of the R_2 line. At $T=1.8 \text{ K}$ and a small excitation power $W=0.05 \text{ W}$ (curve 1) one observes,

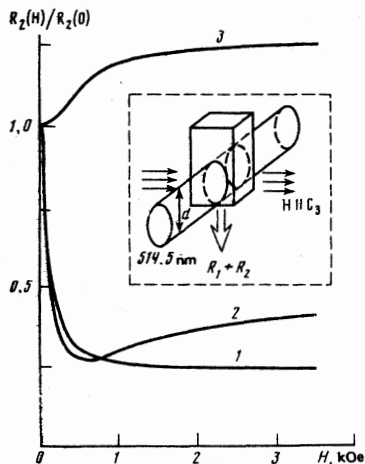


FIG. 1. Dependence of the R_2 -line intensity, normalized to $H=0$, on the magnetic field: 1— $T=1.8$, $W=0.05$; 2— $T=1.8$, $W=1$; 3— $T=4.2 \text{ K}$, $W=0.02 \text{ W}$. Inset: experimental geometry.

in accord with Refs. 3 and 4, a monotonic decrease of $R_2(H)/R_2(0)$ with the field, down to a level ≈ 0.25 in strong fields. The value $\eta = 0.8 \times 10^{-5}$ observed at $W = 0.05 \text{ W}$ exceeds slightly the equilibrium value $\bar{n}_0 \approx 10^{-10}$ at $T=1.8 \text{ K}$, and consequently [see (1)] the value of η is completely governed by the trapping of the nonequilibrium phonons.

On curve 2 of Fig. 1, which corresponds to a high power $W=1 \text{ W}$, a clearly pronounced anomaly is observed, namely R_2H increases in fields¹⁾ $H > 600 \text{ Oe}$. In addition, it is seen that curve 2 decreases more steeply than curve 1, i.e., with increasing W the observed $R_2(H)$ "contour" becomes narrower. A similar tendency was observed in Ref. 13 (in a certain region of W).

Curve 3 of Fig. 1 was obtained at values $T=4.2 \text{ K}$ and $W=0.02 \text{ W}$. Under these conditions, the quantity $\bar{n}_0 \approx 5 \cdot 10^{-5}$ prevails over the first term in (1), due to the trapping of the phonons, and the experimental $R_2(H)/R_2(0)$ dependence (curve 3) turns out to be entirely different than at $T=1.8 \text{ K}$ (curves 1 and 2). The observed increase of $R_2(H)$ of the equilibrium luminescence with saturation in fields $H > 2 \text{ kOe}$ is due to the decrease of the reabsorption of the optical radiation of the R_2 line following its Zeeman splitting.¹⁸ Corrections for free absorption were introduced both in curves 1 and 2 of Fig. 1 and in all the succeeding results.

The points in Fig. 2 show the measurement results in the field region $H \geq 100 \text{ Oe}$ of the anomalous field dependence of $\eta(H)$ at different pumps $W=0.1-1 \text{ W}$. The results are presented in the form of the ratio $\eta(H)/\eta(H=3.5 \text{ kOe})$. Normalization to the value of η in the minimum field $H=3.5 \text{ kOe}$, at which the plots approach saturation (Fig. 1), was chosen for convenience in the comparison with the theoretical calculations (see Sec. 4 below). With this normalization, the curves for different pump powers W do not intersect (in contrast to Fig. 1).

It is seen from Fig. 2 that with increasing W the "depth" of the anomaly $\eta(0.6)/\eta(3.5)$ increases, while its minimum retains its position at $H=0.6 \text{ kOe}$. The quantitative dependence of $\eta(0.6)/\eta(3.5)$ on the pump W is shown in Fig. 3 (by dark circles).

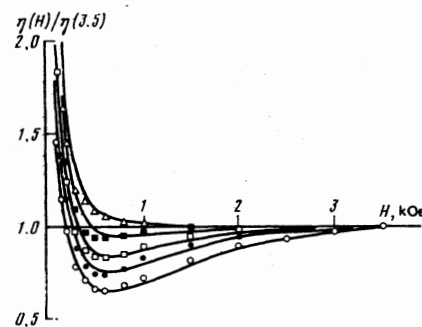


FIG. 2. Dependence of the ratio $\eta = R_2/R_1$, normalized to $H=3.5 \text{ kOe}$, on the magnetic field at various pump powers W : (○—1; ●—0.6; □—0.4; ■—0.2; △—0.1 W). Solid lines—calculation.

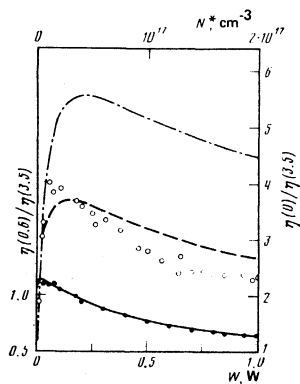


FIG. 3. Dependence of the relative values of η on the pump power. Points—experiment, line—calculation. Dark circles (left-hand ordinate)— $\eta(0.6)/\eta(3.5)$; light circles (ordinate on the right)— $\eta(0)/\eta(3.5)$. Calculated curves for $H_{10c}=15$ Oe (dash-dot) and $H_{10c}=40$ Oe (dashed).

Figure 3 shows also (light circles) the W dependence of the relative value $\eta(0)/\eta(3.5)$ of η in a zero external field. This quantity characterizes the decrease of the trapping in a maximum field compared with zero, and depends monotonically on W .¹⁹ At small W (small N^*) the magnetic field exerts practically no influence and $\eta(0)/\eta(3.5) \approx 1$. With increasing W , the field effect increases rapidly and the ratio $\eta(0)/\eta(3.5)$ reaches a maximum value ≈ 4 (Refs. 3 and 4). With further increase of W , this ratio decreases to ≈ 2 .

Figure 4 shows experimental plots of the absolute value of η vs W in fields $H=0.6$ kOe (position of the minimum) and $H=3.5$ kOe ("saturating" maximum field). These data in conjunction with the relative values of η shown in Figs. 1–3 provide a sufficiently complete picture of the dependence of η on the magnetic field in the interval $0 < H \leq 3.5$ kOe at different pumping powers W .

2. TRAPPING OF RESONANT FLUORESCENCE AND DIFFUSION OF 29 cm^{-1} PHONONS

The laws governing the trapping of 29 cm^{-1} phonons in multiple resonant scattering are determined by the

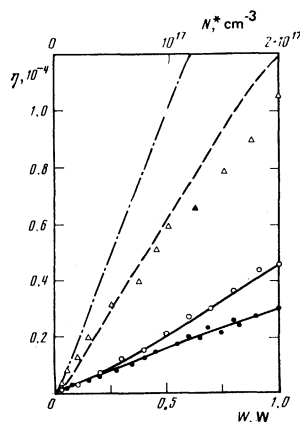


FIG. 4. Dependence of η on the pump power in fields $H=0$ (triangles), $H=0.6$ kOe (dark circles). Calculated curves in fields $H=0.6$ kOe and 3.5 kOe (solid lines), at $H_{10c}=15$ Oe (dash-dot), and $H_{10c}=40$ Oe (dashed).

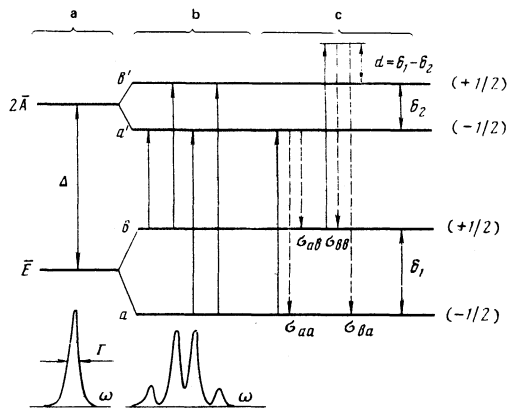


FIG. 5. Scheme of Zeeman splitting of the \bar{E} and $2\bar{A}$ levels, of the resonant transitions, and of the scattering process.

elementary act of phonon scattering by excited Cr^{3+} ions. We consider first the case $H=0$, when there are two levels, \bar{E} and $2\bar{A}$, separated by an energy $\Delta=29 \text{ cm}^{-1}$ [Fig. 5(a)]. The cross section for the resonant scattering of the phonons by a two-level system can be represented in the form^{20,21}

$$\sigma(\omega_0, \omega) \sim \frac{\Gamma^2/4}{(\omega_0 - \Delta)^2 + \Gamma^2/4} \left[\frac{\Gamma_{\parallel}}{\Gamma} \delta(\omega - \omega_0) + \frac{\Gamma_{\perp}}{\Gamma} \frac{\Gamma/2\pi}{(\omega - \Delta)^2 + \Gamma^2/4} \right]. \quad (2)$$

Here ω_0 and ω are the frequencies of the incident and scattered phonons; $\Gamma = \Gamma_{\parallel} + \Gamma_{\perp}$, $\Gamma_{\parallel} = T^{-1}$ is the reciprocal lifetime of the $2\bar{A}$ state (longitudinal width of the line), and Γ_{\perp} is the rate of phase relaxation (transverse width of the field). The latter takes into account the influence exerted on the resonant elastic scattering of 29 cm^{-1} phonons by other channels in the scattering of phonons through the $2\bar{A}$ and \bar{E} states. The quantity Γ_{\perp} can depend on the frequency ω_0 or ω . The first term in the square brackets of (2) corresponds to the elastic process of resonant fluorescence,^{22,23} and the second to the inelastic process, which can be called (in contrast to the first) phonon luminescence. Luminescence is secondary emission from the "prepared" state $2\bar{A}$ and is characterized by absence of phase memory. The resonant fluorescence is the usual resonant scattering via the intermediate quasistationary state $2\bar{A}$, and it proceeds with a definite delay of the phase of the scattered wave; in this sense it is a coherent process.

The trapping mechanism depends essentially on the ratio of the probabilities of the longitudinal (Γ_{\parallel}) and transverse (Γ_{\perp}) relaxation. In the case $\Gamma_{\perp} \gg \Gamma_{\parallel}$ the scattering act comprises, according to (2), stepwise (uncorrelated) absorption and luminescence, in which case the Holstein-Biberman trapping mechanism is effective^{9,10} and leads to the line self-reversal of the typical, e.g., of radiation transport in gases.

The opposite situation $\Gamma_{\perp} \ll \Gamma_{\parallel}$, when the phase relaxation can be neglected, holds for 29 cm^{-1} in ruby.^{4,8} In particular, no role is played by the relaxation Γ_{\perp} due to two-phonon Raman (nonresonant scattering processes, which are responsible for the temperature broadening of the ruby R -lines²⁴: extrapolation of the data of Ref. 24

on the R -line width yields at $T=2$ K a value $\Gamma_1 \approx 1 \text{ sec}^{-1}$. In weakly doped ruby at not too strong trapping (see Sec. 5 below), other phase relaxation mechanisms also become insignificant, particularly those connected with ion-ion interaction, as is confirmed, e.g., by the data of Ref. 25.

Thus, for 29 cm^{-1} phonons at $T=2$ K the scattering (2) on the $\bar{E}-2\bar{A}$ transition is practically purely elastic ($\omega = \omega_0$) (case of resonant fluorescence). The theory of trapping of resonant fluorescence was developed independently by Levinson⁶ and by Malyshev and one of us,⁷ and the so-called spectral transport equations for resonant quanta in crystals were formulated there. Under certain conditions these equations reduce to spatial diffusion of the energy of the electronic excitations and of the phonons. The diffusion coefficient connected with the time delay of the phonons in the scattering and with their ballistic delay between the scattering acts is

$$D_1 = \frac{1}{3} T_1^{-1} k^{-2}(\omega), \quad T_1 = T + [vk(\omega)]^{-1},$$

where $k^{-1}(\omega)$ is the phonon mean free path in resonant scattering, and v is the phonon velocity. The coefficient D_1 comes into play when the trapping time is measured in nonstationary experiments. The diffusion coefficient of the $2\bar{A}$ excitations (more accurately speaking, of the phonons in the scattering state) is

$$D_0(\omega) = \frac{1}{3} T_0^{-1} k^{-2}(\omega), \quad T_0 = T.$$

The coefficient D_0 manifests itself in measurements of the degree of trapping in stationary experiments (see also Ref. 26).

It must be emphasized that the diffusion of the resonant phonon fluorescence has in principle important features that distinguish it as a special quantum phenomenon, in which classical kinetic and quantum wave properties are organically combined. The phenomenon is unique because both the quantum states of the normal crystal vibrations (phonons) and the local purely electronic $2\bar{A}$ state manifest themselves in the multiple scattering process as virtual states. Thus, in particular, no real population of the $2\bar{A}$ level takes place in the elementary act of resonant fluorescence. For a consistent interpretation of the trapping it is important to take into account the fact that the "resonant quanta" pertain in the spectral transport theory^{6,7} not to purely electronic $2\bar{A}$ states or to phonons as normal lattice vibrations, but to $2\bar{A}$ states as phonon-scattering states and to phonons as asymptotic scattering states. The latter are described in the theory of trapping of resonant fluorescence^{6,7} by a Wigner density matrix in the Keldysh representation²⁷ and are specific packets of normal vibrations. The time $[vk(\omega)]^{-1}$ for such packets has the meaning of the free-path time. On the other hand, the total delay time T_1 takes into account both the delay of the phonons in the $\bar{E}-2\bar{A}$ resonant fluorescence and their delay due to the group velocity of the resonance phonons.²⁷ The time T_1 turns out to be numerically equal to the sum of the lifetime T of the electronic $2\bar{A}$ state and the time $[vk(\omega)]^{-1}$, where v is the phonon velocity in the unexcited (nonresonant) region of the crystal.^{6,7,26}

In light of the foregoing, the heuristic notion that the delay time in scattering is the "lifetime T of a resonant quantum in the form of an electronic $2\bar{A}$ excitation" is incorrect. The free-path time $[vk(\omega)]^{-1}$ is likewise not the real "time that the resonant quantum stays as a crystal phonon." In the latter case we would have a spectral broadening of the resonant diffusing quantum, due to the uncertainty of the energy of the crystal vibrations $\hbar vk(\omega)$, whereas the spatial diffusion of the resonant fluorescence is due to elastic scattering and takes place without a change of frequency. In addition, the group velocity of the phonons in a resonant volume differs from v . The equality $T_1 = T + [vk(\omega)]^{-1}$ should therefore be understood as a theoretically deduced relation between the two quantities T_1 and $\{T + [vk(\omega)]^{-1}\}$, whose physical definitions are by far not the same. The same remark holds also for the equality $T_0 = T$. With these remarks taken into account, the detailed balancing principle, which establishes the connection between the spectral densities of the electronic excitations and of the phonons,^{6,26} also assumes a different character under conditions of resonant-fluorescence trapping.

The distinguishing features of the scattering of 29 cm^{-1} phonons in ruby are reflected also in the properties of the optical R_2 radiation, which under conditions of trapping of nonequilibrium phonons cannot be legitimately regarded as luminescence, i.e., as emission from a "prepared" state ($2\bar{A}$). Under these conditions the frequency of the R_2 line is equal to the sum of the frequencies of the phonon and of the transition $\bar{E}-^4A_2$, which differs in principle from the frequency of the $2\bar{A}-^4A_2$ transition. The detected R_2 radiation is consequently the result of a sort of phonon-phonon scattering via the virtual $2\bar{A}$ state.

The theory of diffusion of resonant fluorescence,^{6,7} was confirmed in experiments on the trapping of 29 cm^{-1} phonons in ruby. In particular, the quadratic concentration dependence $\eta \sim N^{*2}$ observed in weak trapping^{4,19} is a direct reflection of the diffusion mechanism of the emergence of 29 cm^{-1} phonons from the volume. Taking the foregoing into account, we neglect in the next section the transverse relaxation, assuming²⁾ $\Gamma_1 = 0$.

3. RESONANT RAMAN SCATTERING OF PHONONS IN A MAGNETIC FIELD AND QUALITATIVE INTERPRETATION OF THE EXPERIMENT

When a magnetic field $H \parallel C_3$ is turned on, the Kramers doublets \bar{E} and $2\bar{A}$ are split, with respective g -factors^{1,28} $g_1 = 2.445$ and $g_2 = 1.5$. As a result, the form factor of the $2\bar{A}-\bar{E}$ transition is transformed into a quartet [Fig. 5(b)] that has resonances at the frequencies $\Delta \pm (\delta_1 \pm \delta_2)/2$, where $\delta_{1,2} = g_{1,2} \mu_B H$. The more intense internal lines of the quartet correspond to transitions without spin flip, and the outer lines correspond to spin flip. For experiments in a magnetic field, the most important is the spectral characteristic of the scattering, and we confine ourselves here therefore to an isotropic approximation (the influence of the anisotropic scattering of 29 cm^{-1} phonons^{29,30} is discussed in Secs. 4 and 5 below).

In contrast to resonant fluorescence of a two-level system [Fig. 5(a)], a system of four Zeeman levels

[Fig. 5(b)] admits, besides elastic scattering, also inelastic scattering with change of the phonon frequency by an amount $\pm\delta_1$. This is resonant Raman scattering (RRS) of phonons. Its distinguishing feature in this case is that a local magnon $\delta_1 = g_1 \mu_B H$ is produced (or vanishes) in the electron system (Cr^{3+} ions). The corresponding differential scattering cross sections can be easily obtained by perturbation theory for second-order processes with allowance for the damping of the intermediate states (see, e.g., Refs. 17 and 20):

$$\begin{aligned} \sigma(\omega_0, \omega) = & p_a [\sigma_{aa} \delta(\omega - \omega_0) + \sigma_{ab} \delta(\omega - \omega_0 + \delta_1)] \\ & + p_b [\sigma_{bb} \delta(\omega - \omega_0) + \sigma_{ba} \delta(\omega - \omega_0 - \delta_1)], \end{aligned} \quad (3)$$

$$\begin{aligned} \sigma_{aa,bb}(\omega_0) = & \sigma_0 \left[\left(\frac{\Gamma^+}{\Gamma^-} \right)^2 \frac{\Gamma^2/4}{[\omega_0 - \Delta \mp (\delta_1 - \delta_2)/2]^2 + \Gamma^2/4} \right. \\ & \left. + \left(\frac{\Gamma^-}{\Gamma^+} \right)^2 \frac{\Gamma^2/4}{[\omega_0 - \Delta \mp (\delta_1 + \delta_2)/2]^2 + \Gamma^2/4} \right], \end{aligned} \quad (3a)$$

$$\begin{aligned} \sigma_{ab,ba}(\omega_0) = & \sigma_0 \left[\frac{\Gamma^2/4}{[\omega_0 - \Delta \mp (\delta_1 - \delta_2)/2]^2 + \Gamma^2/4} \right. \\ & \left. + \frac{\Gamma^2/4}{[\omega_0 - \Delta \mp (\delta_1 + \delta_2)/2]^2 + \Gamma^2/4} \right] \frac{\Gamma^- \Gamma^+}{\Gamma^2}. \end{aligned} \quad (3b)$$

The partial cross sections σ_{aa} and σ_{bb} (respectively “-” and “+” in [3(a)] correspond to elastic channels in scattering, while σ_{ab} and σ_{ba} [“-” and “+” in (3b)] correspond to inelastic channels of RRS with spin flip in the \bar{E} state. By σ_0 in [3(a), (b)] is denoted the cross section for scattering at the line center ($\omega_0 = \Delta$) at $H=0$; p_a and p_b are the populations of the Kramers $\bar{E}_{a,b}$ sublevels ($p_a + p_b = 1$); Γ^+ and Γ^- are the probabilities, per unit time, of spontaneous $2\bar{A} - \bar{E}$ transitions without and with spin flip, respectively, and $\Gamma^+ + \Gamma^- = \Gamma = T^{-1}$. It is known from Ref. 1 that $1/\Gamma^+ + 1/\Gamma^- = 15 \cdot 10^{-9}$ sec, and there are also estimates $\Gamma = (1-3) \times 10^9 \text{ sec}^{-1}$ (Refs. 31, 32) and $\Gamma^-/\Gamma^+ \approx 1/60$ (Ref. 31).

Figure 5(c) shows schematically the scattering processes corresponding to individual partial cross sections in (3). For the sake of clarity, the example illustrated in the figure pertains to the case when the Zeeman splittings exceed the line width ($\delta_{1,2} > \Gamma$), and the frequency ω of the incident phonon is at resonance with one of the spin-allowed transitions ($a-a'$). In fact, both upper intermediate states (a' and b') contribute to each of the four partial cross sections.

We consider now qualitatively the phonon trapping in a magnetic field. Since the RRS is connected with spin-flip transitions, its cross section is of the order of smallness Γ^-/Γ^+ relative to the elastic scattering. For this reason, in the case of weak trapping (small M) the main contribution is made by elastic scattering. In this case a characteristic monotonic decrease of $\eta(H)$ with the field takes place, due to the smearing of the resonance as a result of the Zeeman splitting of the levels^{4,13} (see curves 1 in Figs. 1 and 6).

For sufficiently strong trapping (large M), the RRS is repeated many times and comes into play despite the smallness of Γ^-/Γ^+ . Since the change of the phonon frequency $\pm\delta_1$ in each RRS act is equally probable (at $p_a = p_b$), repeated scattering in a weak field ($\delta_1 \ll \Gamma$) causes

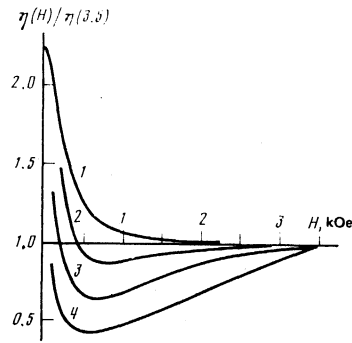


FIG. 6. Calculated dependence of the ratio $\eta = R_2/R_1$, normalized to $H=3.5$ kOe, on the magnetic field for different values of Γ^-/Γ^+ : 1—0; 2—0.02; 3—0.05; 4—1.

spectral diffusion of the phonons.⁶ The frequency discontinuities $|\delta_1|$ increase with increasing field, therefore the decrease of $\eta(H)$ in the field becomes steeper [narrowing of the “resonant contour” $\eta(H)$, Ref. 13].

Of fundamental interest is the strong-field case, when the function $\eta(H)$ changes qualitatively. In this situation ($\delta_1 \gg \Gamma$) the spectral distribution of the trapped phonons is concentrated in the region of the quartet of resonant frequencies $\Delta \pm (\delta_1 \pm \delta_2)/2$ [see Fig. 7(c) below]. Let us note some important properties of the inelastic scattering of phonons in this case, using as an example Fig. 5(c), where the frequency ω_0 of the incident phonon is at resonance with the transition $a-a'$ [$\omega_0 \approx \Delta + (\delta_1 - \delta_2)/2$]. In the Stokes process [σ_{ab} in Fig. 5(c)] there appears a phonon with frequency $\omega_0 - \delta_1$, which is at resonance with another transition ($b-a'$) and consequently can be again effectively scattered. Similar RRS processes contribute

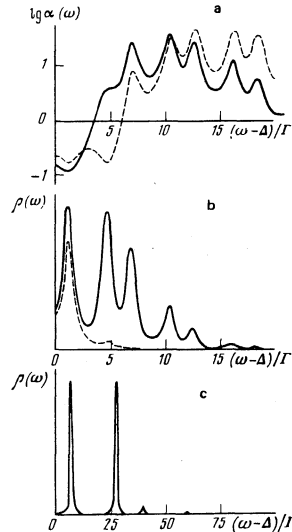


FIG. 7. Spectral functions at $k_0 L = 720$, $\gamma_p L / v = 0.05$; a— $\log \alpha(\omega)$ in a field $H = 0.6$ kOe at $\Gamma^-/\Gamma^+ = 0.05$ (solid line) and $\Gamma^-/\Gamma^+ = 1$ (dashed); b— $\rho(\omega)$ in a field $H = 0.6$ kOe at $\Gamma^-/\Gamma^+ = 0.05$ (the dashed line shows the form factor of the $\bar{E} - 2\bar{A}$ transition); c— $\rho(\omega)$ in a field $H = 3.5$ kOe at $\Gamma^-/\Gamma^+ = 0.05$. The spectral functions can be symmetrically continued into the frequency region $\omega < \Delta$ (it was assumed that $p_a = p_b$).

to equalization of the phonon density among the resonances.⁶ On the other hand, in the anti-Stokes process σ_{ba} , an "off-resonance" phonon $\omega_0 + \delta_1$ appears, with a frequency that exceeds the maximum resonant frequency of the Zeeman quartet. This phonon has a high probability of leaving the excited volume without rescattering. The inelastic processes with production of phonons $\omega_0 \pm \delta_1$, one of which can leave the volume freely and the other is effectively scattered in it, take place for each of the four resonant frequencies ($\omega_0 = \Delta \pm (\delta_1 \pm \delta_2)/2$). Off-resonance phonons can appear here (depending on the position of ω_0) in Stokes or anti-Stokes inelastic scattering. It is obvious that scattering processes with production of off-resonance phonons should decrease the trapping efficiency greatly. If Γ^- and Γ^+ are unequal, the trapping efficiency is decreased also by processes of the first type.

We consider now the magnetic-field dependence of the partial cross sections for phonon scattering. Let, e.g., $\omega_0 = \Delta + (\delta_1 - \delta_2)/2$ [Fig. 5(c)]. It is seen from [3(a), (b)] that the cross sections σ_{aa} and σ_{bb} for the elastic processes, as well as σ_{ab} , for the inelastic process that leads to a redistribution of the density of the phonons within the quartet, are decreased by a factor of two when δ_1 increases from 0 to $\delta_1 \gg \Gamma$. The cross section σ_{ba} for the inelastic Raman process behaves differently and leads to the appearance of off-resonance phonons. In strong fields ($\delta_1, \delta_2 \gg \Gamma$) (the cross section σ_{ba} tends to zero like H^{-2}). This is a manifestation of the "resonance" defect $d = \delta_1 - \delta_2$ which is the characteristic of RRS [see Fig. 5(c)] and increases with increasing H . A similar dependence ($\propto H^{-2}$) is exhibited in strong fields by the cross sections for inelastic scattering with appearance of off-resonance phonons, and in the spectral region of the remaining three transitions ($b - b', a - b', b - a'$). Since these processes undoubtedly lower the degree η of the trapping, their suppression ($\propto H^{-2}$) with increasing H should increase η in the corresponding region of H . This is the qualitative explanation of the experimentally observed nonmonotonic $\eta(H)$ dependence.

4. TRANSPORT EQUATIONS UNDER CONDITIONS OF MULTIPLE RESONANT RAMAN SCATTERING OF 29 cm^{-1} PHONONS

The physical interpretation of the theory of resonant dragging, given in Sec. 2, leads to kinetic premises in the derivation of the equation that governs the process. This classical approach to the theory of multiple scattering from a weakly bound system is well known³³ and is justified if the scatterer density is low enough. In contrast to equations of the Boltzmann type, the departure term in the equation for the radiant transport of electronic excitation is connected exclusively with the natural lifetime T , and this is the distinguishing feature of the collision integral in this equation. The corresponding balance equation takes the form

$$\dot{\Phi}(\mathbf{r}, \omega, t) = -\Gamma\Phi(\mathbf{r}, \omega, t) + S(\mathbf{r}, \omega, t) + \Lambda(\mathbf{r}, \omega, t), \quad (4a)$$

where $\Phi(\mathbf{r}, \omega, t)$ is the spectral density of the $2\bar{A}$ excitations,⁷ or more accurately speaking the density of the phonons in the scattering state. This function has the meaning of a source of phonons of frequency ω , scatter-

ed by ions at the macroscopic point \mathbf{r} at the instant of time t , and can be normalized the local density of the $2\bar{A}$ excitations

$$\int \Phi(\mathbf{r}, \omega, t) d\omega = n(\mathbf{r}, t),$$

which is directly connected with the measured integrated intensity of the R_2 line:

$$R_2 \sim \int n(\mathbf{r}, t) d^3r.$$

The function $\Lambda(\mathbf{r}, \omega, t)$ is the spectral density of the phonon pumping, and is connected in this case with the form factor $I(\omega)$ of the $2\bar{A}-\bar{E}$ transition. The collision integral $S(\mathbf{r}, \omega, t)$ is due to rescattering, by the ions at the macroscopic point \mathbf{r} of the phonons that were scattered by all the remaining ions at the instants of time preceding t :

$$S(\mathbf{r}, \omega, t) = \Gamma N \int d^3r' \int d\omega' \int dt' \Phi(\mathbf{r}', \omega', t') \frac{\sigma(\omega', \omega)}{4\pi|\mathbf{r}-\mathbf{r}'|^2} \times \exp\left\{-|\mathbf{r}-\mathbf{r}'| \left[k(\omega') + \frac{\gamma_p}{v} \right]\right\} \delta\left(t-t' - \frac{|\mathbf{r}-\mathbf{r}'|}{v}\right). \quad (4b)$$

In this expression, the Bouguer exponential factor takes into account the extinction of the phonons between the scattering acts, as a result of both the resonant scattering

$$k(\omega') = N^* \sigma(\omega'), \quad \sigma(\omega') = \int \sigma(\omega', \omega'') d\omega'',$$

and of the anharmonic damping with the time constant γ_p^{-1} ; the δ function takes into account the retardation of the phonons; $\sigma(\omega', \omega)/4\pi|\mathbf{r}-\mathbf{r}'|^2$ is the impact solid angle at which the cross section $\sigma(\omega', \omega)$ at the point \mathbf{r} is seen from the point \mathbf{r}' . Following Sec. 3, we have confined ourselves in [4(a), (b)] to the case of isotropic scattering.

Expressions [4(a), (b)] give the sought transport equation.³ In the presence of RRS in a field $H \neq 0$, this equation agrees with the relations, obtained in Ref. 6, between the spectral densities of the phonons and the electronic excitations, and can be derived in this case from these relations (see the Appendix). The region of applicability of (4) is limited by the condition $k(\omega)\lambda \ll 1$ (Ref. 7) or, equivalently, $|n(\omega) - 1| \ll 1$, where $n(\omega)$ is the complex refractive index of the resonant medium. Since $\lambda \approx 80 \text{ \AA}$, $\sigma_0 \approx 0.5 \cdot 10^{-13} \text{ cm}^2$, this limits the density to $N^* \ll 10^{20} \text{ cm}^{-3}$. In this approximation we neglect, in particular, the interference of the phonons scattered by different ions (the so-called scattering by a weakly bound system³³). In addition, no due allowance is made in (4) for the temporal dispersion of the spectra $\sigma(\omega', \omega)$ and $k(\omega')$, which is connected with the dynamics of the elementary scattering acts.²⁶ This remark is significant for pulsed experiments. In the stationary regime $\dot{\Phi} = 0$ and Eq. (4) is valid for an arbitrary form of the resonant-scattering cross sections $\sigma(\omega', \omega)$. In particular, it is valid also in the presence of phase relaxation $\Gamma_1 \neq 0$. If $\sigma(\omega', \omega) = \sigma(\omega')I(\omega)$, then the variables \mathbf{r} and ω in (4) separate with a corresponding factorization of the function

$$\Phi(\mathbf{r}, \omega, t) = n(\mathbf{r}, t)I(\omega),$$

with the local density $n(\mathbf{r}, t)$ satisfying the Holstein equa-

tion,⁹ which is thus a particular case of (4). For pure elastic scattering

$$\sigma(\omega', \omega) = \sigma(\omega') \delta(\omega - \omega')$$

Eq. (4) coincides with the equation obtained in Ref. 7 for the trapping of resonant fluorescence.⁷

As applied to the conditions of this experiment, Eq. (4) was considered in the regime of stationary homogeneous pumping $\Lambda(\mathbf{r}, \omega, t) = \Gamma I(\omega)$. The cross section (3), which includes the RRS, was used for $\sigma(\omega', \omega)$. Since the degree of trapping is determined by the smallest linear dimension of the excited volume, this volume, in the form of a cylinder of diameter $d \approx 1.3$ mm and length 3 mm, was approximated by a flat layer of thickness L (the influence of the shape of the volume at $k_0 L \gg 1$ is not connected with the RRS channels, i.e., it is the same as in the ordinary diffusion problem³⁵). The L -containing parameters $k_0 L$ and $\gamma_p L/v$ were chosen by comparison with experiment. Thus, we arrive from (4) at the equation

$$\Phi(z, \omega) = I(\omega) + \int_0^z dz' \int d\omega' \Phi(z', \omega') K(z' - z, \omega', \omega) \quad (5a)$$

with an integral-exponential kernel

$$K(z, \omega', \omega) = \frac{1}{2} N \sigma(\omega', \omega) \int_1^\infty \exp\{-y|z| [k(\omega') + \frac{\gamma_p}{v}]\} \frac{dy}{y}. \quad (5b)$$

In the case of elastic scattering it coincides formally with the inhomogeneous Milne equation. Equation (5) was solved numerically with a computer. At a normalization $\int I(\omega) d\omega = 1$, the function $\Phi(z, \omega)$ in [5(a)] is connected with the number M in (1) by

$$\int_0^L \frac{dz}{L} \int d\omega \Phi(z, \omega) = M + 1.$$

We have considered also the transport equation with allowance for the anisotropic resonant scattering of longitudinal phonons in ruby.^{4,30,36} In the assumed experimental geometry (see Fig. 1), multiple resonant scattering leads to emission of longitudinal 29 cm⁻¹ phonons from the volume in a narrow cone along the C_3 axis.^{4,29} To ascertain the role of the anisotropic trapping in experiments in a magnetic field, we considered Eq. (5a) with a kernel

$$K(z, \omega', \omega) = \frac{3}{8} N \sigma(\omega', \omega) \int_0^\infty \exp\left\{-|z| \frac{u}{(1+u)^{1/2}} \left[k(\omega') + \frac{\gamma_p}{v}\right]\right\} \frac{u^2 du}{(1+u)^3}, \quad (5c)$$

corresponding to the case of "dipole" directivity pattern ($\sin^2\theta$) of the phonon scattering near the C_3 axis.³⁶

Account was also taken in the calculations of the inhomogeneity of the distribution of the excited Cr³⁺ ions in the volume of the beam and in its vicinity (the light halo), which acts as a surface layer that reflects the phonons into the interior of the volume. In the numerical solution of (5) we solved a specially selected factor α in the relation

$$\frac{d}{dz} \Phi(z, \omega) = \alpha k(\omega) \Phi(z, \omega),$$

that corresponds to the boundary condition of the differential diffusion problem. The coefficient α was chosen to fit the dependence of $\eta(0.6)/\eta(3.5)$ on W (Fig. 3),

which is sensitive to its value in the region of medium and small W . Satisfactory agreement with experiment is obtained at $\alpha = 0.6 \pm 0.2$ (theoretically, in the case of an abrupt boundary and a uniform distribution we have $\alpha \approx 1.4$). The parameter Γ^-/Γ^+ is not very sensitive to the choice of α ($\alpha \neq 0$ within certain limits), since it is connected mainly with the nonmonotonic behavior of $\eta(H)$ (Fig. 6), which at large W is practically independent of α . The boundary conditions that take into account the inhomogeneity of $N^*(r)$ make it possible thus to obtain agreement between the family of the calculated $\eta(H)/\eta(3.5)$ curves with the experimental ones (Fig. 2) in a wider interval of W . We note that in experiments with very weak pumping (see footnote 5 below) a linear $\eta(N^*)$ dependence was observed, corresponding to $\alpha \approx 0.8$. In light of the foregoing, an attempt to take into account the shape of the volume would be an exaggeration of the accuracy, since the inhomogeneity of N^* is a more substantial factor.

5. COMPARISON OF CALCULATION WITH EXPERIMENT. DISCUSSION

The results of the calculations of the value of η and of other quantities that characterize the multiple scattering are shown in Figs. 2-4, 6, and 7. In these calculations we obtained or used the concrete values of the physical parameters Γ^-/Γ^+ , T , γ_p , $p_{a,b}$, as well as $k_0 L$ ($k_0 = N^* \sigma_0$).

Figure 6 shows the theoretical plot of $\eta(H)/\eta(3.5)$ at different values of Γ^-/Γ^+ . At $\Gamma^- = 0$ the scattering is elastic⁴¹ and the corresponding $\eta(H)$ takes the form of a resonance contour (curve 1 of Fig. 6). An $\eta(H)$ dependence of this type is observed in experiment in the case of weak trapping, when the influence of the RRS is minimal (Fig. 1, curve 1). With increasing Γ^-/Γ^+ , the shape of the calculated $\eta(H)$ curve changes, a minimum appears at $H = 0.6$ kOe, and the nonmonotonic behavior of $\eta(H)$ is pronounced stronger the larger the ratio Γ^-/Γ^+ . Thus, the solution of the transport equation that takes into account multiple RRS of the phonons confirms the qualitative interpretation, discussed in Sec. 3, of the phenomenon.

Figure 2 shows theoretical plots of $\eta(H)/\eta(3.5)$ at $\Gamma^-/\Gamma^+ = 0.05$ and at different values of the parameter $k_0 L$, corresponding to the given laser power. The calculated curves agree with the experimental ones. Satisfactory agreement is obtained also for the dependence of the depth of the anomaly $\eta(0.6)/\eta(3.5)$ on W (Fig. 3). The theoretical and experimental dependences of $\eta(W)$ in a fixed field (sufficiently strong: $H = 0.6$ and 3.5 kOe) are also in agreement (Fig. 4).

In a zero external field ($H = 0$), however, there is a noticeable discrepancy between theory and experiment both for the function $\eta(W)$ (Fig. 4) and for the ratio $\eta(0)/\eta(3.5)$ (Fig. 3). We note that in the calculation of the properties of trapping in a zero magnetic field we took into account the presence of internal local magnetic fields $H_{loc} = 15$ Oe (Ref. 1). Figures 3 and 4 show the calculated curves for $H_{loc} = 15$ Oe (dash-dot), as well as for the value $H_{loc} = 40$ Oe (dashed). Although the last

variant agrees best with experiment, the value $H_{loc} = 40$ Oe is apparently not realistic.

A possible cause of the disagreement with the calculation at $H=0$ is the neglect, in the scattering, of the interference due to the Kramers degeneracy of the $2\bar{A}$ level. In the case of multiple scattering, in interference leads to diffusion of the coherence,³⁷ and under multiple-scattering conditions it influences, in addition, the contribution of the RRS and the efficiency of the spectral diffusion. In this sense, the trapping mechanism turns out to be simpler in strong fields (where coherence in the $2\bar{A}$ state is violated) than at $H=0$. The quantity $\eta(H)$, in particular, is therefore normalized to the value in a strong field $H=3.5$ kOe (Fig. 2).

The agreement between theory and experiment (Fig. 2) in region $H \geq 0.5$ kOe, which covers the section where $\eta(H)$ is anomalous and nonmonotonic, confirms convincingly the decisive role of the RRS of the phonons in trapping in a magnetic field. The multiple RRS results in a substantial redistribution of the phonons over the frequencies, and is this which is responsible for the anomalous behavior of $\eta(H)$ (Fig. 2). The latter is an integrated characteristic of the distribution function. The spectral functions calculated directly under conditions of multiple RRS are shown in Figs. 7(a), (b), (c).

The function $\alpha(\omega)$ [Fig. 7(a)] is defined in terms of the average number of scattering acts by

$$M = \int M_0(\omega) \alpha(\omega) I(\omega) d\omega,$$

where $M_0(\omega)$ is the number of scatterings of a monochromatic phonon of frequency ω in pure elastic scattering. The function $\alpha(\omega)$ is connected in a definite manner with the solution of Eq. (5) and takes into account the influence of the inelastic scattering channels. It provides a clear representation of the phonon frequency distribution. In the frequency region where $\alpha(\omega) < 1$, the spectral density decreases as a result of inelastic scattering, while in the region where $\alpha(\omega) > 1$ it increases; on the other hand if $\Gamma^- = 0$, i. e., there is no inelastic scattering, then $\alpha(\omega) = 1$. Figure 7(a) shows a plot of $\log \alpha(\omega)$ calculated for $H = 0.6$ kOe at two values of $\Gamma^-/\Gamma^+ = 0.5$ and 1. It is seen that the multiple RRS produces effectively nonresonant phonons corresponding to "overtones" at frequencies separated from the resonant frequencies by amounts that are multiples of δ_1 . In the resonance region, the spectral density decreases ($\log \alpha < 0$). At $\Gamma^-/\Gamma^+ = 1$ it comes into play at the frequencies of both transitions ($a-a'$ and $a-b'$) and is due exclusively to the transfer into the region of the overtones. At $\Gamma^-/\Gamma^+ = 0.05$, where there is an additional redistribution of the phonons among the spin-allowed and spin-forbidden resonances, we have $\alpha < 1$ only in the region of the allowed $a-a'$ transition.

Figures 7(b) and 7(c) show the volume-averaged spectral distribution of the trapped phonons for $\Gamma^-/\Gamma^+ = 0.05$. It is seen that in a field $H = 0.6$ kOe, corresponding to the minimum of $\eta(H)$ (Fig. 2), the phonon densities in the region of both resonances and the overtones are comparable in value [Fig. 7(b)]. In a strong field $H = 3.5$ kOe [Fig. 7(c)], which corresponds to sat-

uration of $\eta(H)$ (Figs. 2 and 6), the densities ρ of both resonances become equalized and in addition the overtones vanish almost completely. This is due to the suppression ($\propto H^{-2}$), in a strong magnetic field, of the cross section for scattering with production of off-resonance phonons. Equalization of the phonon density in the spectral region of the spin-allowed and spin-forbidden transitions takes place only in the case of strong trapping and is caused according to [3(b)] by the equality of the cross sections of the corresponding RRS channels.

The experimental and theoretical relations (Figs. 2, 3, and 4) agree at definite values of the parameters that enter in the calculated formulas. The ratio of the probabilities of the $2\bar{A}-E$ transitions with and without spin flip turned out to be $\Gamma^-/\Gamma^+ = 0.05$, which is three times larger than the theoretical value.³¹ Using the obtained ratio Γ^-/Γ^+ and the known value $1/\Gamma^+ + 1/\Gamma^- = 15$ nsec (Ref. 1), we get $\Gamma^+ = 1.4 \times 10^9$ sec⁻¹, $\Gamma^- = 0.07 \times 10^9$ sec⁻¹, and a $2\bar{A}$ -level lifetime $T = (\Gamma^+ + \Gamma^-)^{-1} = 0.7$ nsec (kinetic experiments³² yielded $T = 1.1$ nsec). From the expression⁵⁾ for η_0 at $T = 0.7$ nsec and $\tau_{R_1} = 4-5$ msec we estimate the pumping branching coefficient at $\beta \approx 0.5$, which agrees approximately with the data³² obtained at $\lambda_{exc} = 580$ nm. In the estimate we chose for the ratio of the oscillator strengths of the lines R_2 and R_1 the ratio $f_2/f_1 \approx 1$, which was measured by us in the experimental geometry (Fig. 1).

From a comparison of the experiment and the calculation we estimated also the width $\Delta\nu$ of the phonon line of the $2\bar{A}-E$ transition, which turned out to be uniquely connected with the position of the minimum $H = 0.6$ kOe of the $\eta(H)/\eta(3.5)$ dependence (see Fig. 2). The obtained value $\Delta\nu = 0.012$ cm⁻¹ agrees with the result of a direct measurement of the form factor of the $E-2\bar{A}$ transition.³⁸ The $2\bar{A}$ -level lifetime $T = 0.7$ nsec corresponds to the homogeneous width of the 0.008 cm⁻¹ level, and correspondingly its inhomogeneous width⁶⁾ is approximately equal to 0.01 cm⁻¹.

As for the parameter $\gamma_\beta L/v$ connected with the anharmonic decay of the phonons, it was found that its influence on the properties of the trapping in the magnetic field, in the interval $0 < \gamma_\beta < (4 \mu\text{sec})^{-1}$, can be compensated by a suitable choice of the parameter $k_0 L = \sigma_0 N^* L$, which is likewise not known beforehand with the required accuracy (see footnote 8 in this connection). For example, $k_0 L$ is found to equal 540 at $\gamma_\beta = 0$ ($W = 1$ W). On the other hand if we put $\gamma_\beta L/v = 0.05$, where $v = 0.7 \times 10^6$ cm/sec and $L = 1.3$ mm, and $\gamma_\beta = (4 \mu\text{sec})^{-1}$, then $k_0 L$ is equal to 720 at $W = 1$ W. In both cases, the agreement with experiment is satisfactory (the calculated curves shown in all the figures pertain to the case $\gamma_\beta L/v = 0.05$ and $k_0 L = 720$ at $W = 1$ W). In both cases satisfactory agreement with experiment is obtained (the calculated curves shown in all the figures pertain to the case $\gamma_\beta L/v = 0.05$ and $k_0 L = 720$ at $W = 1$ W). Plots of $\eta(H)$ and $\eta(W)$ identical to those observed are obtained also in calculations that take anisotropic effects into account, even though the values of η calculated from (5a) and (5b) for the same values of $k_0 L$ differ by an approximate factor of 2. The last circumstance agrees with Refs. 4 and 30, where special

investigations were made of the anisotropic properties in the trapping of 29 cm^{-1} phonons. Thus, since we do not know accurately the correspondence between the scales of W and k_0L , it is impossible to draw on the basis of experiments in a magnetic field unambiguous conclusions concerning the value of the anharmonic constant⁷⁾ γ_p , nor concerning the influence of the anisotropy of the scattering. In these experiments, as already noted, it is primarily and characteristically that the frequency dependences of the cross section manifests itself. The value of the parameter k_0L obtained with allowance for the anisotropy in accord with (5c) seems to be the most correct. At $0 < \gamma_p < (4\ \mu\text{sec})^{-1}$ it turns out to equal $(1-1.5)\times 10^3$ (at $W=1\text{ W}$). Therefore at⁸⁾ $N=(1-3)\times 10^{17}\text{ cm}^{-3}$ and $L=1.3\text{ mm}$ we obtain the estimate $\sigma_0=(0.3-1.0)\times 10^{-13}\text{ cm}^2$. It agrees with the expression $\sigma_0\approx\lambda^2\Gamma/2\pi\Delta\nu$ for the cross section for resonant scattering at an average wavelength $\lambda\approx 80\ \text{\AA}$ of the 29 cm^{-1} phonon.

We have also undertaken calculations of the $\eta(H)$ dependence under conditions of Holstein trapping,^{9,10} when $\sigma(\omega_0, \omega)=\sigma(\omega_0)I(\omega)$. In this case the value of η was found to be practically independent of the field in the region $H < 0.5\text{ kOe}$, to increase slightly to a level $\eta(H)/\eta(0)\approx 1.1$ at $H=2\text{ kOe}$, and to fall off in very strong fields, $3-6\text{ kOe}$, to the level $0.7-0.5$ (which depends on Γ^-/Γ^+). The large value of the field, which decreases η substantially (and increases with N^*), is connected with the Holstein-trapping characteristic frequency ω^* by the condition $k(\omega^*)L=1$. In the case of strong trapping (large N^*) the frequency ω^* lies far on the line wing, so that the corresponding field is strong. The described calculated behavior of $\eta(H)$ differs greatly from the observed behavior (Figs. 1 and 2).

Thus, the experiments performed in a magnetic field confirm convincingly that in ruby with low chromium density the trapping of the 29 cm^{-1} phonons at $T\approx 2\text{ K}$ and under moderate excitation ($N^* < 10^{17}\text{ cm}^{-3}$) is due to multiple scattering of the type of resonant fluorescence and RRS. This is caused by the negligibly low rate of phase relaxation in the 2E state of Cr^{3+} under these conditions. The phonon-trapping picture can, however, change with increasing temperature, with increasing rate of phase relaxation, as well as with the increasing density N^* of the excited ions. In the latter case, the width of the \bar{E} level, due to the same multiple scattering of the 29 cm^{-1} phonons, increases. This width is connected with the probability of the phonon-induced $\bar{E}-2\bar{A}$ transition, which is equal to $\Gamma\eta\approx 10^2 M$. The result is inelastic Holstein scattering of the phonons, of the luminescence type, in (2). This mechanism of phase relaxation of the \bar{E} level is probably the cause of the broadening of the $\eta(H)$ "contour" with increasing N^* in the case of strong trapping.^{3,13}

6. RRS OF 29 cm^{-1} PHONONS AND SPIN-LATTICE RELAXATION IN THE \bar{E} (2E) STATE OF Cr^{3+} IONS IN RUBY

The spin-lattice relaxation in the \bar{E} state of the Cr^{3+} ions in ruby at low temperatures is due to the Orbach-

Aminov mechanism,^{16,17} which is connected with the presence of the nearby $2\bar{A}$ level.¹ The RRS of 29 cm^{-1} phonons with spin flip in the \bar{E} state (σ_{ab}, σ_{ba}) are the elementary acts of this relaxation. It follows thus from the results of the present paper that the Orbach-Aminov relaxation in ruby at $T=1.8\text{ K}$ is a two-phonon RRS, rather than the $\bar{E}_{a,b}-2\bar{A}$ one-phonon process of absorption of a 29 cm^{-1} phonon followed by the decay $2\bar{A}-\bar{E}_{a,b}$ (Refs. 1 and 31). In the latter case, the Holstein-Bi-berman trapping mechanism would be in action.

Strongly dependent on the spin relaxation is the population ratio p_a/p_b of the Kramers $\bar{E}_{a,b}$ sublevels that influence the scattering cross section (3) and the degree of phonon trapping. The populations p_a and p_b can differ in magnitude. The reason is the unequal Boltzmann population of the Zeeman sublevels $\pm 1/2$ and $\pm 3/2$ of the ground state 4A_2 , which leads to unequal pumping of the $\bar{E}_{a,b}$ sublevels because of the spin-memory effect⁴¹ and, in addition, to a difference between their radiative times on account of optical reabsorption.⁴² The trapping of the 29 cm^{-1} phonons is accompanied by spin relaxation in the \bar{E} state and contributes therefore to the equalization of p_a and p_b .¹ In the general case, the problem of finding the values of p_a and p_b consists of obtaining a self-consistent solution of the corresponding balance equations for the $\bar{E}_{a,b}$ sublevels and for the phonon transport equation under conditions of multiple resonant scattering. In our experiments, however, which were performed in moderate fields ($H\leq 3.5\text{ kOe}$), the Boltzmann factor does not manifest itself in the 4A_2 state. This is seen, in particular, from the observed invariance of $\eta(W\geq 0.1\text{ W})$ when the crystal temperature is raised from 1.5 to 3 K . This is also confirmed by an estimate of the spin-relaxation time $T_s^{-1}\approx 4\Gamma^-\Gamma^+\eta/\Gamma$, which is numerically equal to the radiative time τ_{R1} of the \bar{E} level at $\eta\approx 10^{-6}$. On the other hand, if $\eta\gg 10^{-6}$, as is the case in the present study, the spin manages to "flip" many times during the lifetime of the E level. The population equality $p_a=p_b$ is then established, as was indeed assumed in all the calculations.

We consider now qualitatively the question of trapping under conditions when $p_a\neq p_b$. The form factor of the $2\bar{A}-\bar{E}$ transition is then transformed into an asymmetrical quartet. In weak fields ($\delta_1, \delta_2\ll\Gamma$) a directed spectral transfer of the phonons arises in this case. It proceeds more rapidly than "ordinary" spectral diffusion. In a strong field, a larger role is assumed by inelastic scattering with redistribution of the phonons among the resonances. In this case (since the phonons are transferred to a weakly absorbed resonance) the degree of trapping can decrease noticeably, as observed in experiment.^{14,15} In Ref. 43, an appreciable deviation of p_a/p_b from unity was directly observed in very strong fields ($H=30\text{ kOe}$). It appears that an important role was played in the experiments of Ref. 43 by the already mentioned mechanism of accelerated release of the phonons as a result of inelastic scattering. It leads to a decrease of η and consequently of the rate of spin relaxation T_s^{-1} , thereby contributing to preservation of the inequality $p_a\neq p_b$ under conditions of a strong Zeeman splitting of the 4A_2 state and of the spin memory when pumped.

In conclusion, the authors thank I. B. Levinson and V. I. Perel' for helpful discussions and remarks.

APPENDIX

In the derivation of the integral transport equation from the relations of Ref. 6 it is convenient to change over to the spectral balance relation (3.20) of Ref. 6 to the space-time Fourier transform:

$$[-i\bar{\omega} + i\nu\kappa\mathbf{k} + \gamma_p + \nu k(\omega)]s(\omega, \mathbf{q}, \mathbf{k}, \bar{\omega}) = \beta\bar{G}(\mathbf{k}, \omega) \frac{\Delta(\omega, \mathbf{q})}{\rho_0} \frac{\Phi(\omega)}{\delta\omega} + \frac{\Delta(\omega, \mathbf{q})}{\rho_0} \Gamma \int A(\mathbf{k}, \omega', \bar{\omega}) w(\omega', \omega) d\omega'. \quad (\text{A1})$$

Here $A(\mathbf{k}, \omega', \bar{\omega})$ and $s(\omega, \mathbf{q}, \mathbf{k}, \bar{\omega})$ are the Fourier transforms of the spectral density of the $2\bar{A}$ excitations and of the phonons of the mode \bar{q} , which were introduced in Ref. 6:

$$A(\mathbf{k}, \omega', \bar{\omega}) = \Phi(\omega') \int d^3r \int dt e^{i\bar{\omega}t - i\mathbf{k}\mathbf{r}} F(\mathbf{r}, \omega', t), \quad (\text{A2a})$$

$$s(\omega, \mathbf{q}, \mathbf{k}, \bar{\omega}) = \int d^3r \int dt e^{i\bar{\omega}t - i\mathbf{k}\mathbf{r}} s(\omega, \mathbf{q}, \mathbf{r}, t). \quad (\text{A2b})$$

In (A1) the unit vector is $\kappa = \mathbf{q}/q$; the quantities γ_p^{-1} , $\nu k(\omega)$, β , $T = \Gamma^{-1}$ are designated in (6) by τ_0 , $\gamma^*(\omega)$, η , τ respectively; the function $w(\omega', \omega)$ in (A1) is the normalized scattering spectrum $\sigma(\omega', \omega)/\sigma(\omega')$, which is expressed in terms of the quantity $R(\omega', \omega)$ of Ref. 6 in the following manner

$$w(\omega', \omega) = \Phi^{-1}(\omega') \left\{ R(\omega', \omega) + \delta(\omega - \omega') \left[\Phi(\omega) - \int R(\omega, \omega'') d\omega'' \right] \right\}. \quad (\text{A3})$$

Using (A1) as well as the spectral relation (3.16) of Ref. 6, we arrive at the following integro-differential equation:

$$\left(\frac{\partial}{\partial t} + \Gamma \right) A(\mathbf{r}, \omega, t) = k(\omega) \int d^3r' \int dt' K_{\omega}(\mathbf{r} - \mathbf{r}', t - t') \times \left[\beta\bar{G}(\mathbf{r}', t') \frac{\Phi(\omega)}{\delta\omega} + \Gamma \int d\omega' A(\mathbf{r}', \omega', t') w(\omega', \omega) \right], \quad (\text{A4})$$

$$K_{\omega}(\mathbf{r}, t) = \int \frac{d\bar{\omega}}{2\pi} e^{-i\bar{\omega}t} \int \frac{d^3k}{(2\pi)^3} e^{i\mathbf{k}\mathbf{r}} \int d\Omega_x \left[-i\frac{\bar{\omega}}{\nu} + i\kappa\mathbf{k} + \frac{\gamma_p}{\nu} + k(\omega) \right]^{-1} = \delta\left(t - \frac{r}{\nu}\right) \exp\left\{-r\left[k(\omega) + \frac{\gamma_p}{\nu}\right]\right\} \frac{1}{4\pi r^2}. \quad (\text{A5})$$

This is the kernel usually encountered in the theory of multiple scattering [see, in particular, (36) of Ref. 7]. It is obviously connected with the diverging radial wave of the scattered particles (in this case, phonons) with account taken of their extinction, but without allowance for the delay due to scattering and to the change of the group velocity of the phonons in the dispersive medium (resonant volume). Equation (A4) is therefore meaningful, strictly speaking, only under stationary conditions, when the delay in scattering is insignificant [just as the delay factor $\delta(t - r/\nu)$ in (A5)]. This restriction is due to the fact that the Laplace transform

$$\int_0^{\infty} e^{-t} K_{\omega}(\mathbf{r}, t) dt$$

corresponds to the square of a two-particle pseudopotential⁷ only if we neglect in the latter the temporal dispersion of the cross sections for coherent forward scattering and incoherent scattering [see expressions (33) and (34b) of Ref. 7]. This dispersion is responsible for the delay in scattering and for the retardation (or advance, if $|\omega - \Delta| < \Gamma/2$) connected with the group

velocity.²⁶ In elastic and inelastic phonon scattering in the case of a weak magnetic field, when $\delta_1, \delta_2 \ll \Gamma$, the use of the kernel (A5) is justified,²⁶ as is therefore the change from Eq. (34) to (35)–(40) in Ref. 7. Therefore the equations of the spectral diffusion of the phonons⁶ are therefore also valid under stationary as well as nonstationary experimental conditions.

For the kinetics of multiple multichannel scattering of the RRS type of 29 cm^{-1} phonons in a strong magnetic field ($\delta_1 \geq \Gamma$), Eq. (A4) with kernel (A5) does not hold, for the reason given above (this constitutes the singularity of the gross-structure time scale in multiple resonant scattering²⁶). But this equation is valid for the stationary experiment reported in the present paper, as are also Eqs. (4a) and (4b), which were written for simplicity without allowance for the retardation of the phonons in the coherent and incoherent phonon scattering events: the latter can be rewritten, using (A5), in the form

$$\left(\frac{\partial}{\partial t} + \Gamma \right) \Phi(\mathbf{r}, \omega, t) = \Lambda(\mathbf{r}, \omega, t) + \Gamma \int d^3r' \int d\omega' \int dt' \times k(\omega') \Phi(\mathbf{r}', \omega', t') K_{\omega}(\mathbf{r} - \mathbf{r}', t - t') w(\omega', \omega) \quad (\text{A6})$$

[the dynamic function $\Phi(\mathbf{r}, \omega, t)$ must not be confused with the form factor $\Phi(\omega)$ of Ref. 6]. We note that the function $A(\mathbf{r}, \omega, t) = \Phi(\omega)F(\mathbf{r}, \omega, t)$ of Ref. 6 and $\Phi(\mathbf{r}, \omega, t)$ in (A6), which determined the spectral density of the $2\bar{A}$ excitations with respect to absorption and scattering of phonons, respectively, are connected as follows: (A7a)

$$A(\mathbf{r}, \omega, t) = \Gamma k(\omega) \int_{-\infty}^t e^{-\Gamma(t-t')} dt'' \int d^3r' \int dt' \Phi(\mathbf{r}', \omega, t') K_{\omega}(\mathbf{r} - \mathbf{r}', t'' - t'), \quad (\text{A7b})$$

$$\Phi(\mathbf{r}, \omega, t) = \int_{-\infty}^t e^{-\Gamma(t-t')} \Lambda(\mathbf{r}, \omega, t'') dt'' + \int A(\mathbf{r}, \omega', t) w(\omega', \omega) d\omega'.$$

From this we can show that Eqs. (A4) and (A6) are equivalent, and the ratio of the pumps in these equations is given by

$$\Lambda(\mathbf{r}, \omega, t) = \beta G(\mathbf{r}, t) \Phi(\omega) / \delta\omega,$$

where $\Phi(\omega)/\delta\omega = I(\omega)$; the spectrum $\Phi(\omega)$ was normalized in accordance with Ref. 6 at the center of the line $\Phi(\omega = \Delta) = 1$.

The equations given in the Appendix enable us to trace the connection between two approaches in the theory of multiple resonant scattering. One of them⁶ is based on the spectral balance relations of the electronic excitations and of the radiation, derived by the Keldysh method. In the second approach⁷ multiple scattering is regarded as a many-body problem, the bodies being coupled by a two-particle pseudopotential (optical in the case of resonant scattering in Ref. 7). This method was transferred to the theory of multiple potential scattering (see Ref. 33) from the many-body problem (the Brueckner-particle pseudopotential).

¹On one of the curves of Ref. 13 one can note a similar non-monotonicity, but it is very weak and is not discussed by the authors.

²We shall return in Sec. 5 to the question of transverse relaxation of the levels \bar{E} and $2\bar{A}$ in light of the results of experiments in a magnetic field.

- ³A similar equation was considered in the theory of trapping of optical secondary emission.³⁴
- ⁴Isotropic elastic scattering leads to spatial diffusion of the phonons if $\gamma_p = 0$. Then the number M is equal to $M = \int M(\omega)I(\omega)d\omega$, $M(\omega) \sim L^2k^2(\omega)$. Therefore $\eta(3.5)/\eta(0) = 0.25$, as is in fact observed for weak trapping (Fig. 3). We note in this connection the faster than linear increase of $\eta(W)$ at $H = 3.5$ kOe (Fig. 4). This seems to point to a manifestation of spatial diffusion under conditions when the contribution of the RRS is suppressed in a magnetic field. This is also evidence of a sufficiently large anharmonic lifetime of the phonons (see footnote 7 below). The linearity of $\eta(W)$ at $H = 0$ is explained qualitatively, if not quantitatively, by the spectral diffusion due to local fields.^{15,35}
- ⁵We used in the calculations the value $R_2/R_1 \equiv \eta_0$ for hot R_2 luminescence; this value was specially measured by us under extremely weak excitation, when there is no trapping [$M = 0$ and $\eta_0 = f_2\beta T / 1\tau_{R1}$ in Eq. (1)]. The measurements yielded $\eta_0 = 0.8 \cdot 10^{-7}$.
- ⁶The inhomogeneous broadening enters in the theory via the $I(\omega)$ spectrum, and also via the absorption and scattering cross sections $\sigma(\omega')$ and $\sigma(\omega', \omega)$, which are averaged over the inhomogeneous distribution. The forms of Eqs. (4) and (5) are not changed thereby.
- ⁷In light of the results of experiments on the damping of ballistic 29 cm^{-1} phonons in ruby,³⁹ which point to a long time $\lambda_p^{-1} > 4 \mu\text{sec}$, the role of the anharmonic damping of the phonons seems to be overestimated in the discussion of Refs. 4, 12, and 40.
- ⁸Theoretically $N^* = 5 \times 10^{17} \text{ cm}^{-3}$ at $W = 1 \text{ W}$, $d = 1.3 \text{ mm}$, and $\lambda = 514 \text{ nm}$. The loss to reflection decreases N^* by almost one-half. Therefore N^* can be estimated only at $(1-3) \times 10^{17} \text{ cm}^{-3}$. The values on the N^* scale of Fig. 6 of Ref. 4 are too high (in the W scale, the curve on Fig. 6 of Ref. 4 coincides with the data on Fig. 4 of the present paper).
- ¹S. Geschwind, G. E. Devlin, R. L. Cohen, and S. R. Chinn, Phys. Rev. **A137**, 1087 (1965).
- ²K. F. Renk and J. Deisenhofer, Phys. Rev. Lett. **26**, 764 (1971).
- ³J. I. Dijkhuis, A. Van der Pol, and H. W. de Wijn, *ibid.* **37**, 1554 (1976).
- ⁴A. A. Kaplyanskii, S. A. Basoon, and V. L. Shekhtman, Light Scattering in Solids, J. L. Birman, H. Z. Cummins, and K. K. Rebane, eds., 1979, p. 95.
- ⁵R. S. Meltzer and J. E. Rives, Phys. Rev. Lett. **38**, 421 (1977).
- ⁶I. B. Levinson, Zh. Eksp. Teor. Fiz. **75**, 234 (1978) [Sov. Phys. JETP **48**, 117 (1975)].
- ⁷V. A. Malyshev and V. L. Shekhtman, Fiz. Tverd. Tela (Leningrad) **20**, 2915 (1978) [Sov. Phys. Solid State **20**, 1684 (1978)].
- ⁸A. V. Akimov, S. A. Basun, A. A. Kaplyanskii, R. A. Titov, and V. L. Shekhtman, *ibid.* **19**, 3704 (1977) [**19**, 2159 (1977)].
- ⁹T. Holstein, Phys. Rev. **72**, 1212 (1947).
- ¹⁰L. N. Biberman, Zh. Eksp. Teor. Fiz. **17**, 416 (1947).
- ¹¹A. A. Kaplyanskii, S. A. Basun, V. A. Rachin, and R. A. Titov, Pis'ma Zh. Tekh. Fiz. **1**, 628 (1975) [Sov. Tech. Phys. Lett. **1**, 281 (1975)].
- ¹²R. S. Meltzer and J. E. Rives, in: Lattice Dynamics, M. Balkanski, ed., Paris, 1978, p. 77.
- ¹³J. I. Dijkhuis and H. W. de Wijn, Phys. Rev. **B20**, 1884 (1979).
- ¹⁴S. A. Basun, A. A. Kaplyanskii, and V. L. Shekhtman, Fiz. Tverd. Tela (Leningrad) **23**, 3694 (1981) [Sov. Phys. Solid State **23**, 2149 (1981)].
- ¹⁵A. A. Kaplyanskii, S. A. Basoon, and V. L. Shekhtman, J. de Phys. **42**, C6-462 (1981).
- ¹⁶R. Orbach, Proc. Roy. Soc. **A264**, 458 (1961).
- ¹⁷L. K. Aminov, Zh. Eksp. Teor. Fiz. **42**, 783 (1962) [Sov. Phys. JETP **15**, 547 (1962)].
- ¹⁸N. S. Menon and A. W. Nolle, Phys. Rev. **B4**, 3890 (1971).
- ¹⁹J. I. Dijkhuis and H. W. de Wijn, Sol. St. Comm. **31**, 39 (1979).
- ²⁰V. Hizhnyakov and I. Tehver, Phys. Stat. Sol. **21**, 755 (1967).
- ²¹D. L. Huber, Phys. Rev. **178**, 93 (1969).
- ²²W. Heitler, The Quantum Theory of Radiation, Oxford, 1954.
- ²³V. Weisskopf, Ann. Phys. (Leipzig) **9**, 23 (1931).
- ²⁴D. E. McCumber and M. J. Sturge, J. Appl. Phys. **34**, 1682 (1963).
- ²⁵P. E. Jessop and A. Szabo, Phys. Rev. Lett. **45**, 1712 (1980).
- ²⁶V. L. Shekhtman, Fiz. Tverd. Tela (Leningrad) **24** (1982) [Sov. Phys. Solid State **24** (*sic*) (1982)].
- ²⁷L. V. Keldysh, Zh. Eksp. Teor. Fiz. **47**, 1515 (1964) [Sov. Phys. JETP **20**, (1965)].
- ²⁸S. Sugano and I. Tsujikawa, J. Phys. Soc. Jpn. **13**, 899 (1958).
- ²⁹A. A. Kaplyanskii, S. A. Basun, V. A. Rachin, and R. A. Titov, Pis'ma Zh. Eksp. Teor. Fiz. **21**, 438 (1975) [JETP Lett. **21**, 200 (1975)].
- ³⁰S. A. Basun, A. A. Kaplyanskii, and V. L. Shekhtman, Pis'ma Zh. Eksp. Teor. Fiz. **30**, 275 (1979) [JETP Lett. **30**, 255 (1979)].
- ³¹M. Blume, R. Orbach, A. Kiel, and S. Geschwind, Phys. Rev. **A139**, 314 (1965).
- ³²J. E. Rives and R. S. Meltzer, Phys. Rev. **B16**, 1808 (1977).
- ³³M. L. Goldberger and K. M. Watson, Collision Theory, Wiley, 1964.
- ³⁴V. A. Malyshev and V. L. Shekhtman, Abstracts, 6th All-Union Conf. on Spectroscopy of Activated Crystals, Krasnodar, 1979, p. 190.
- ³⁵V. A. Malyshev and V. L. Shekhtman, Fiz. Tverd. Tela (Leningrad) **24** (1982) [Sov. Phys. Solid State **24** (*sic*) (1982)].
- ³⁶V. A. Malyshev and V. L. Shekhtman, Opt. Spektrosk. **46**, 800 (1979) [Opt. Spectrosc. **46**, 446 (1979)].
- ³⁷M. I. D'yakonov and V. I. Perel', Zh. Eksp. Teor. Fiz. **47**, 1483 (1964) [Sov. Phys. JETP **20**, 997 (1965)].
- ³⁸H. Lengfellner, G. Pauli, W. Heisel, and K. F. Renk, Appl. Phys. Lett. **29**, 566 (1976).
- ³⁹S. A. Basun and A. A. Kaplyanskii, Fiz. Tverd. Tela (Leningrad) **22**, 3500 (1980) [Sov. Phys. Solid State **22**, 2055 (1980)].
- ⁴⁰K. F. Renk and J. Peckenzell, J. de Phys. **33**, Suppl. C4, 103 (1972).
- ⁴¹G. E. Imbusch and S. Geschwind, Phys. Rev. Lett. **17**, 238 (1966).
- ⁴²F. Varsanyi, D. L. Wood, and A. L. Schawlow, *ibid.* **3**, 544 (1959).
- ⁴³J. I. Dijkhuis and H. W. de Wijn, Phys. Rev. **B20**, 3615 (1979).

Translated by J. G. Adashko